Class-DE$_{\mathrm{M}}$ Tuned Power Amplifier

Tsuyoshi Inaba, *Student Member, IEEE*, and Hirotaka Koizumi, *Member, IEEE*

***Abstract*—This paper proposes a Class-DE$_{\mathrm{M}}$ tuned power amplifier. The proposed amplifier achieves zero-voltage switching (ZVS), zero-voltage derivative switching (ZVDS), and zero-current switching (ZCS) at turning-ON, and ZVS, ZVDS, ZCS, and zero-current derivative switching at turning-OFF. Therefore, the switching losses are extremely low, which is suitable for high-frequency operation. Moreover, the switch voltage stress is low, which is no more than its input voltage. A proposed amplifier was designed, built, and tested. The measured power conversion efficiency was 93.2% under the condition of the main input voltage of 46.8 V, the operating frequency of 1 MHz, and the output power of 4.87 W.**

***Index Terms*—Class-DE, Class-E, Class-E$_{\mathrm{M}}$, tuned power amplifier.**

I. Introduction

In RECENT years, due to the advancement of wireless communication systems, communication devices are required to be high performance, low cost, and miniaturized. To downsize such devices, miniaturizing the passive components of the radio frequency (RF) power amplifiers is needed. To meet the demand, such amplifiers are required to operate in high frequency with high efficiency [1], [2]. However, higher frequency causes more switching losses.

A Class-D voltage-switching tuned power amplifier [3]–[6], which is one of the classes of RF tuned power amplifiers [7]–[9], realizes high-efficiency operation up to several hundred kilohertz owing to zero-current switching (ZCS). Another advantage of the amplifier is the low peak voltage of the switching devices, which is equal to the input voltage. However, the switches turn ON and OFF at high dv/dt, which increases switching losses in high switching frequency.

A Class-E amplifier [10]–[12] realizes high-efficiency operation up to several megahertz owing to zero-voltage switching (ZVS), zero-voltage derivative switching (ZVDS), and ZCS at the turning-ON instant. One drawback of the amplifier is the high switch voltage stress, which is about 3.56 times higher than the input voltage at the on-duty ratio $D = 0.5$. Another problem of the Class-E amplifier is current jump at turning-OFF.

As a circuit that combines the advantages of the Class-D amplifier and the Class-E amplifier, Class-DE high-efficiency tuned power amplifiers [13]–[15] are proposed. The Class-DE amplifier has a similar topology to the Class-D tuned power

Manuscript received September 6, 2017; revised January 4, 2018 and February 15, 2018; accepted March 4, 2018. Date of publication March 21, 2018; date of current version November 19, 2018. Recommended for publication by Associate Editor R. Zane. *(Corresponding author: Tsuyoshi Inaba.)*

The authors are with the Tokyo University of Science, Tokyo 125-8585, Japan (e-mail:

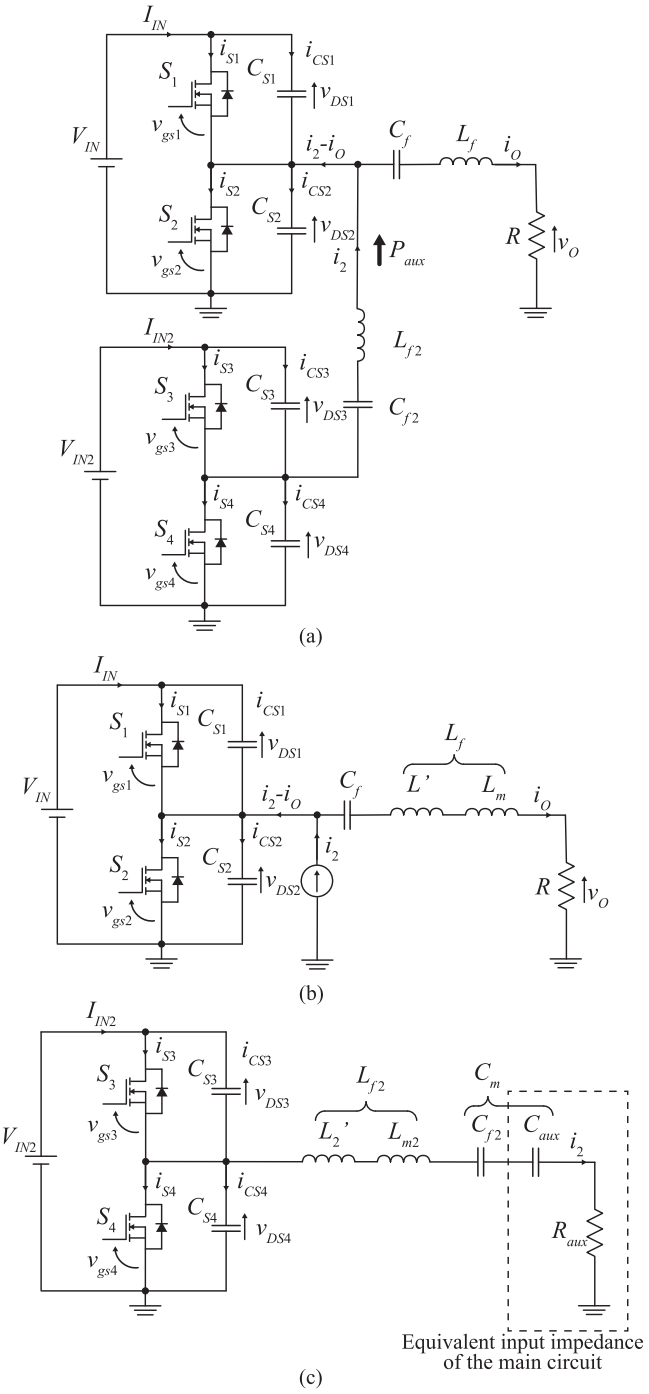

Fig. 1. Class-DE$_{\rm M}$ tuned power amplifier. (a) Overall circuit. (b) Equivalent circuit of the main circuit. (c) Equivalent circuit of the auxiliary circuit.

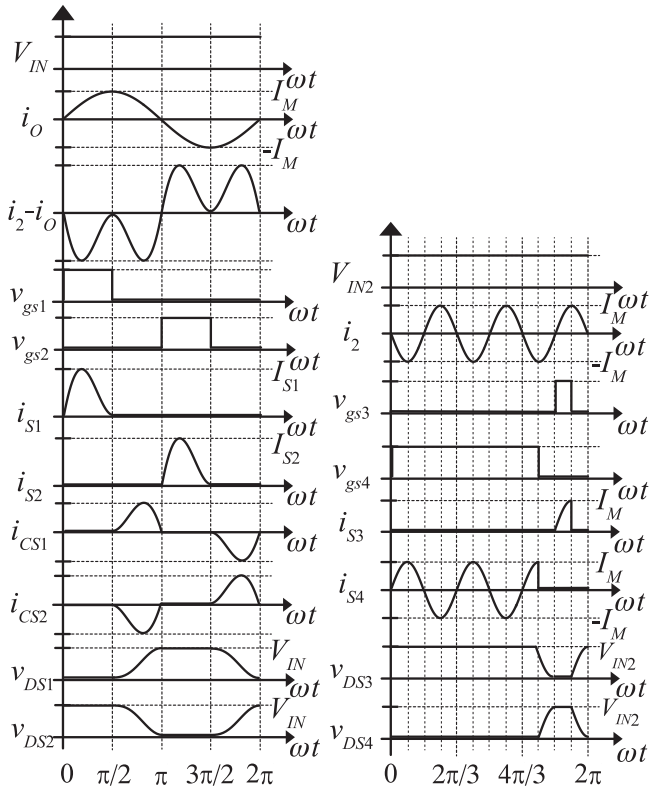

Fig. 2. Ideal waveforms of the Class-DE$_{\rm M}$ tuned power amplifier.

auxiliary circuit. Fig. 1(b) shows the main circuit, which consists of an input voltage $V_{\rm IN}$, two switches S_1 and S_2, two shunt capacitors C_{S1} and C_{S2}, a series-resonant circuit L_f–C_f, and a load resistance R. The inductor L_f can be regarded as a series connection of an inductor L' and an inductor L_m. In this equivalent circuit, the auxiliary circuit is replaced with an ideal ac current source i_2, which supplies the third-order harmonic component of the operating frequency f of the main circuit. Fig. 1(c) shows the auxiliary circuit. The auxiliary circuit operates as a Class-DE frequency multiplier [27], which consists of an input voltage $V_{\rm IN2}$, two switches S_3 and S_4, two shunt capacitors C_{S3} and C_{S4}, a series-resonant circuit L_{f2}–C_m, and a load resistance $R_{\rm aux}$. The resistance $R_{\rm aux}$ and a capacitor $C_{\rm aux}$ is the equivalent impedance of the main circuit. The inductor L_{f2} can be regarded as a series connection of an inductor L_2' and an inductor L_{m2}. When the switches S_3 and S_4 are driven at an operating frequency f, the series-resonant circuit L_2'–C_m is tuned to the third-order harmonic $3f$, and L_{m2} is an additional inductance to provide a phase angle ϕ_2. The capacitor C_m can be regarded as a series connection of a capacitor C_{f2} and the capacitor $C_{\rm aux}$.

The ideal waveforms for the Class-DE$_{\rm M}$ tuned power amplifier are shown in Fig. 2, where $V_{\rm IN}$ is the input voltage, i_O is the output current, i_2–i_O is the differential current, $v_{\rm gs1}$ and $v_{\rm gs2}$ are the gate–source voltages of switches S_1 and S_2, respectively, i_{S1} and i_{S2} are the switch currents, $i_{\rm CS1}$ and $i_{\rm CS2}$ are the currents through shunt capacitances C_{S1} and C_{S2}, respectively, and $v_{\rm DS1}$ and $v_{\rm DS2}$ are the drain–source voltages of switches S_1 and S_2, respectively. In the auxiliary circuit, $V_{\rm IN2}$ is the input voltage, i_2 is the injection current, $v_{\rm gs3}$ and $v_{\rm gs4}$ are the gate–source voltages of switches S_3 and S_4, respectively, i_{S3} and i_{S4} are the switch currents, and $v_{\rm DS3}$ and $v_{\rm DS4}$ are the drain–source voltages of switches S_3 and S_4, respectively.

A. Analysis of the Class-DE$_{\rm M}$ Tuned Power Amplifier

The Class-DE$_{\rm M}$ amplifier is analyzed based on the following assumptions.

1) Switches S_1 and S_2 turn ON and OFF instantaneously. The switches have an OFF-resistance $r_{\rm OFF}$ for the OFF-state and an on-resistance $r_{\rm ON}$ for the ON-state, which are infinite and zero, respectively.
2) All passive elements have no equivalent series resistance (ESR).
3) The loaded quality factor Q_1 of the series-resonant circuit L'–C_f tuned to the operation frequency f is high enough to make the output current in sinusoidal waveform.
4) Shunt capacitances C_{S1} and C_{S2} include parasitic drain–source capacitance of switches S_1 and S_2.
5) The loaded quality factor Q_2 of the series-resonant circuit L_2'–C_m tuned to the third-order harmonic of the operation frequency $3f$ is high enough to make the injection current i_2 in sinusoidal waveform.

The output current i_O is

$$i_O = I_O \sin(\omega t + \phi_1) \tag{1}$$

where I_O is the amplitude, ω is the angular operating frequency that satisfies the relationship of $\omega = 2\pi f$, and ϕ_1 ($0 \le \phi_1 \le 2\pi$) is the phase angle of the output current. The injection current i_2 is

$$i_2 = I_2 \sin(\omega_3 t + \phi_2) \tag{2}$$

where I_2 is the amplitude, ω_3 is the angular frequency of 3ω, and ϕ_2 ($0 \le \phi_2 \le 2\pi$) is the phase angle difference of the injection current i_2. By Kirchhoff's voltage and current laws, we have

$$v_{\rm DS1} + v_{\rm DS2} = V_{\rm IN} \tag{3}$$

$$i_{S1} + i_{\rm CS1} = i_{S2} + i_{\rm CS2} + i_O - i_2. \tag{4}$$

In this circuit, ZVS and ZVDS conditions are achieved at turning-ON and turning-OFF

$$v_{\rm DS1}\left(\frac{\pi}{2}\right) = v_{\rm DS1}(2\pi) = v_{\rm DS2}(\pi) = v_{\rm DS2}\left(\frac{3}{2}\pi\right) = 0 \tag{5}$$

$$\left.\frac{dv_{\rm DS1}(\omega t)}{d(\omega t)}\right|_{\omega t=\frac{\pi}{2}} = \left.\frac{dv_{\rm DS1}(\omega t)}{d(\omega t)}\right|_{\omega t=2\pi} = \left.\frac{dv_{\rm DS2}(\omega t)}{d(\omega t)}\right|_{\omega t=\pi} = \left.\frac{dv_{\rm DS2}(\omega t)}{d(\omega t)}\right|_{\omega t=\frac{3}{2}\pi} = 0. \tag{6}$$

The ZCS condition is achieved at turning-ON and turning-OFF

$$i_{S1}(0) = i_{S1}\left(\frac{\pi}{2}\right) = i_{S2}(\pi) = i_{S2}\left(\frac{3}{2}\pi\right) = 0. \tag{7}$$

ZCDS conditions are achieved at turning-OFF

$$\left.\frac{di_{S1}(\omega t)}{d(\omega t)}\right|_{\omega t=\frac{\pi}{2}} = \left.\frac{di_{S2}(\omega t)}{d(\omega t)}\right|_{\omega t=2\pi} = 0. \tag{8}$$

The Class-DE$_{\rm M}$ amplifier operation is divided into four states by the state of switches S_1 and S_2.

1) State 1 [$0 \le \omega t \le \pi/2$]*:* In state 1, switch S_1 is ON and switch S_2 is OFF. The drain–source voltages $v_{\rm DS1}$ and $v_{\rm DS2}$ and the switch current i_{S2} are

$$v_{\rm DS1} = 0 \tag{9}$$

$$v_{\rm DS2} = V_{\rm IN} \tag{10}$$

$$i_{S2} = 0. \tag{11}$$

From (10), the current through the shunt capacitor $i_{\rm CS2}$ is

$$i_{\rm CS2} = \omega C_{S2}\frac{dv_{\rm DS2}}{d(\omega t)} = \omega C_{S2}\frac{dV_{\rm IN}}{d(\omega t)} = 0. \tag{12}$$

Similarly, the current through the shunt capacitor $i_{\rm CS1}$ is

$$i_{\rm CS1} = 0. \tag{13}$$

From (1), (2), and (4), we have

$$i_{S1} = i_O - i_2 = I_O \sin(\omega t + \phi_1) - I_2 \sin(\omega_3 t + \phi_2). \tag{14}$$

Applying the ZCDS condition (8) to (14), we obtain

$$\left.\frac{di_{S1}(\omega t)}{d(\omega t)}\right|_{\omega t=\frac{\pi}{2}} = I_O \sin\phi_1 + 3I_2 \sin\phi_2 = 0. \tag{15}$$

2) State 2 [$\pi/2 \le \omega t \le \pi$]*:* In state 2, switch S_1 is OFF and switch S_2 is OFF. The switch currents i_{S1} and i_{S2} are

$$i_{S1} = i_{S2} = 0. \tag{16}$$

From (4) and (16), we have

$$-i_{\rm CS1} + i_{\rm CS2} = -i_O + i_2. \tag{17}$$

From (1)–(3) and considering that the capacitor currents $i_{\rm CS1}$ and $i_{\rm CS2}$ are, respectively, $i_{\rm CS1} = \omega C_{S1} dv_{\rm DS1}/d(\omega t)$ and $i_{\rm CS2} = \omega C_{S2} dv_{\rm DS2}/d(\omega t)$, we derive

$$-\omega C_{S1}\frac{d(V_{\rm IN} - v_{\rm DS2})}{d(\omega t)} + \omega C_{S2}\frac{dv_{\rm DS2}}{d(\omega t)} = -I_O \sin(\omega t + \phi_1) + I_2 \sin(\omega_3 t + \phi_2). \tag{18}$$

From (18), we have

$$\frac{dv_{\rm DS2}}{d(\omega t)} = \frac{-1}{\omega(C_{S1}+C_{S2})}\left[I_O \sin(\omega t+\phi_1) - I_2 \sin(\omega_3 t+\phi_2)\right]. \tag{19}$$

Applying the ZVDS condition (6) to (19), we obtain

$$\left.\frac{dv_{\rm DS2}(\omega t)}{d(\omega t)}\right|_{\omega t=\pi} = \frac{1}{\omega(C_{S1}+C_{S2})}(I_O \sin\phi_1 - I_2 \sin\phi_2) = 0. \tag{20}$$

Similarly, we have

$$\left.\frac{dv_{\rm DS1}(\omega t)}{d(\omega t)}\right|_{\omega t=\frac{\pi}{2}} = \frac{1}{\omega(C_{S1}+C_{S2})}(I_O \cos\phi_1 + I_2 \cos\phi_2) = 0. \tag{21}$$

From (15), (20), and (21), we have

$$\begin{cases} 0 = I_O \sin\phi_1 + 3I_2 \sin\phi_2 \\ 0 = I_O \sin\phi_1 - I_2 \sin\phi_2 \\ 0 = I_O \cos\phi_1 + I_2 \cos\phi_2. \end{cases} \tag{22}$$

Giving the ranges of the phase angles ϕ_1 and ϕ_2 as $0 \le \phi_1 \le 2\pi$ and $0 \le \phi_2 \le 2\pi$, and assuming that $I_O = I_2 = I_M$, two solutions

$$\begin{cases} \phi_1 = 0, & \phi_2 = \pi \\ \phi_1 = \pi, & \phi_2 = 0 \end{cases} \tag{23}$$

are derived. When we choose $\phi_1 = \pi$ and $\phi_2 = 0$, the differential current i_2–i_O conducts the body diode of switch S_2 in state 1. Therefore,

$$\phi_1 = 0, \;\; \phi_2 = \pi \tag{24}$$

is a solution suitable for the operation. Substituting (24) into (19), we obtain

$$\frac{dv_{\text{DS2}}}{d(\omega t)} = \frac{-I_M}{\omega(C_{S1} + C_{S2})} \left(\sin \omega t + \sin 3\omega t\right). \tag{25}$$

From (25), we have

$$\begin{aligned} v_{\text{DS2}} &= -\frac{I_M}{\omega(C_{S1} + C_{S2})} \int_{\frac{\pi}{2}}^{\omega t} \left(\sin \omega t + \sin \omega_3 t\right) d(\omega t) \\ &\quad + v_{\text{DS2}}\left(\frac{\pi}{2}\right) \\ &= \frac{I_M}{3\omega(C_{S1} + C_{S2})} \left(3\cos \omega t + \cos 3\omega t\right) + V_{\text{IN}}. \end{aligned} \tag{26}$$

Applying ZVS condition (5) to (26), we obtain

$$V_{\text{IN}} = \frac{4I_M}{3\omega(C_{S1} + C_{S2})}. \tag{27}$$

Therefore, from (26), and (27), the drain–source voltages v_{DS1} and v_{DS2} for state 2 are

$$v_{\text{DS2}}(\omega t) = \frac{3}{4} V_{\text{IN}} \left(\cos \omega t + \frac{1}{3}\cos \omega_3 t + \frac{4}{3}\right) \tag{28}$$

$$\begin{aligned} v_{\text{DS1}}(\omega t) &= V_{\text{IN}} - v_{\text{DS2}}(\omega t), \\ &= -\frac{3}{4} V_{\text{IN}} \left(\cos \omega t + \frac{1}{3}\cos \omega_3 t\right). \end{aligned} \tag{29}$$

The capacitor current i_{CS1} is

$$i_{\text{CS1}} = \frac{i_O - i_2}{2} = \frac{I_M}{2}\left(\sin \omega t + \sin \omega_3 t\right). \tag{30}$$

And the capacitor current i_{CS2} is

$$i_{\text{CS2}} = -\frac{i_O - i_2}{2} = -\frac{I_M}{2}\left(\sin \omega t + \sin \omega_3 t\right). \tag{31}$$

From (30), we have

$$\begin{aligned} v_{\text{DS1}} &= \frac{1}{\omega C_{S1}} \int_{\frac{\pi}{2}}^{\omega t} i_{\text{CS1}} d(\omega t) + v_{\text{DS1}}\left(\frac{\pi}{2}\right) \\ &= -\frac{I_M}{2\omega C_{S1}} \left(\cos \omega t + \frac{1}{3}\cos \omega_3 t\right). \end{aligned} \tag{32}$$

Similarly, from (31),

$$\begin{aligned} v_{\text{DS2}} &= \frac{1}{\omega C_{S2}} \int_{\frac{\pi}{2}}^{\omega t} i_{\text{CS2}} d(\omega t) + v_{\text{DS2}}\left(\frac{\pi}{2}\right) \\ &= \frac{I_M}{2\omega C_{S2}} \left(\cos \omega t + \frac{1}{3}\cos \omega_3 t\right) + V_{\text{IN}}. \end{aligned} \tag{33}$$

Applying the ZVS condition (5) to the above equation, we obtain

$$\begin{aligned} v_{\text{DS2}}(\pi) &= -\frac{2I_M}{3\omega C_{S2}} + V_{\text{IN}} = 0 \\ \iff V_{\text{IN}} &= \frac{2I_M}{3\omega C_{S2}}. \end{aligned} \tag{34}$$

From (32), we have

$$v_{\text{DS1}}(\pi) = \frac{2I_M}{3\omega C_{S1}} = V_{\text{IN}}. \tag{35}$$

In addition, from (34) and (35), we have

$$C_S = C_{S1} = C_{S2} = \frac{2I_M}{3\omega V_{\text{IN}}} \tag{36}$$

where C_S is a shunt capacitance in common.

3) State 3 [$\pi \le \omega t \le 3\pi/2$]: In state 3, switch S_1 is OFF and switch S_2 is ON. The drain–source voltages v_{DS1} and v_{DS2} are

$$v_{\text{DS1}} = V_{\text{IN}} \tag{37}$$

$$v_{\text{DS2}} = 0. \tag{38}$$

And the switch current i_{S1} is

$$i_{S1} = 0. \tag{39}$$

The currents flowing through the shunt capacitors i_{CS1} and i_{CS2} are

$$i_{\text{CS1}} = i_{\text{CS2}} = 0. \tag{40}$$

The switch current i_{S2} is

$$i_{S2} = -i_O + i_2 = -I_M\left(\sin \omega t + \sin \omega_3 t\right). \tag{41}$$

When $\omega t = 3\pi/2$,

$$i_{S2}\left(\frac{3}{2}\pi\right) = -I_M\left(\sin\frac{3}{2}\pi + \sin\frac{9}{2}\pi\right) = 0. \tag{42}$$

Therefore, the ZCS condition (7) is satisfied.

4) State 4 [$3\pi/2 \le \omega t \le \pi$]: In state 4, switch S_1 is OFF and switch S_2 is OFF

$$i_{S1} = i_{S2} = 0. \tag{43}$$

From (4) and (43), we have

$$i_{\text{CS1}} - i_{\text{CS2}} = i_O - i_2 = I_M\left(\sin \omega t + \sin \omega_3 t\right). \tag{44}$$

Thus, we have

$$\begin{aligned} \omega C_{S1}\frac{dv_{\text{DS1}}}{d(\omega t)} - \omega C_{S2}\frac{d(V_{\text{IN}} - v_{\text{DS1}})}{d(\omega t)} \\ = I_M\left(\sin \omega t + \sin \omega_3 t\right) \\ \frac{dv_{\text{DS1}}}{d(\omega t)} = \frac{I_M}{\omega(C_{S1} + C_{S2})}\left(\sin \omega t + \sin \omega_3 t\right). \end{aligned} \tag{45}$$

Therefore, we have

$$\begin{aligned} v_{\mathrm{DS1}} &= \frac{I_M}{\omega(C_{S1}+C_{S2})}\int_{\frac{3}{2}\pi}^{\omega t}(\sin\omega t+\sin\omega_3 t)\,d(\omega t) \\ &\quad + v_{\mathrm{DS1}}\left(\frac{3}{2}\pi\right) \\ &= \frac{-I_M}{3\omega(C_{S1}+C_{S2})}(3\cos\omega t+\cos\omega_3 t)+V_{\mathrm{IN}}. \end{aligned} \tag{46}$$

Applying the ZVS condition (5) to (46), we obtain

$$\begin{aligned} & v_{\mathrm{DS1}}(2\pi) = -\frac{4I_M}{3\omega(C_{S1}+C_{S2})}+V_{\mathrm{IN}}=0, \\ \iff & V_{\mathrm{IN}} = \frac{4I_M}{3\omega(C_{S1}+C_{S2})}. \end{aligned} \tag{47}$$

From (46) and (47), the drain–source voltage v_{DS1} is

$$v_{\mathrm{DS1}} = -\frac{3}{4}V_{\mathrm{IN}}\left(\cos\omega t+\frac{1}{3}\cos\omega_3 t-\frac{4}{3}\right). \tag{48}$$

And the drain–source voltage v_{DS2} is

$$v_{\mathrm{DS2}} = V_{\mathrm{IN}} - v_{\mathrm{DS1}} = \frac{3}{4}V_{\mathrm{IN}}\left(\cos\omega t+\frac{1}{3}\cos\omega_3 t\right). \tag{49}$$

From the above, the voltage and the current waveforms are summarized shown as follows:

$$v_{\mathrm{DS1}}(\omega t) = \begin{cases} 0, & \left[0<\omega t\le\frac{\pi}{2}\right] \\ -\frac{3}{4}V_{\mathrm{IN}}\left(\cos\omega t+\frac{1}{3}\cos\omega_3 t\right), & \left[\frac{\pi}{2}<\omega t\le\pi\right] \\ V_{\mathrm{IN}}, & \left[\pi<\omega t\le\frac{3\pi}{2}\right] \\ -\frac{3}{4}V_{\mathrm{IN}}\left(\cos\omega t+\frac{1}{3}\cos\omega_3 t-\frac{4}{3}\right), & \left[\frac{3\pi}{2}<\omega t\le 2\pi\right] \end{cases} \tag{50}$$

$$v_{\mathrm{DS2}}(\omega t) = \begin{cases} V_{\mathrm{IN}}, & \left[0<\omega t\le\frac{\pi}{2}\right] \\ \frac{3}{4}V_{\mathrm{IN}}\left(\cos\omega t+\frac{1}{3}\cos\omega_3 t+\frac{4}{3}\right), & \left[\frac{\pi}{2}<\omega t\le\pi\right] \\ 0, & \left[\pi<\omega t\le\frac{3\pi}{2}\right] \\ \frac{3}{4}V_{\mathrm{IN}}\left(\cos\omega t+\frac{1}{3}\cos\omega_3 t\right), & \left[\frac{3\pi}{2}<\omega t\le 2\pi\right] \end{cases} \tag{51}$$

$$i_{S1}(\omega t) = \begin{cases} I_M\left(\sin\omega t+\sin\omega_3 t\right), & \left[0<\omega t\le\frac{\pi}{2}\right] \\ 0, & \left[\frac{\pi}{2}<\omega t\le\pi\right] \\ 0, & \left[\pi<\omega t\le\frac{3\pi}{2}\right] \\ 0, & \left[\frac{3\pi}{2}<\omega t\le 2\pi\right] \end{cases} \tag{52}$$

$$i_{S2}(\omega t) = \begin{cases} 0, & \left[0<\omega t\le\frac{\pi}{2}\right] \\ 0, & \left[\frac{\pi}{2}<\omega t\le\pi\right] \\ -I_M\left(\sin\omega t+\sin\omega_3 t\right), & \left[\pi<\omega t\le\frac{3\pi}{2}\right] \\ 0, & \left[\frac{3\pi}{2}<\omega t\le 2\pi\right]. \end{cases} \tag{53}$$

The input current I_{IN} is equal to the averaged value of the switch current i_{S1}. From (52), we have

$$\begin{aligned} I_{\mathrm{IN}} &= \frac{1}{2\pi}\int_0^{2\pi} i_{S1}\,d(\omega t) \\ &= \frac{I_M}{2\pi}\int_0^{\frac{\pi}{2}}(\sin\omega t+\sin\omega_3 t)\,d(\omega t) = \frac{2I_M}{3\pi}. \end{aligned} \tag{54}$$

Substituting (47) into (54), the input current I_{IN} is

$$I_{\mathrm{IN}} = \frac{2I_M}{3\pi} = \frac{\omega(C_{S1}+C_{S2})V_{\mathrm{IN}}}{2\pi}. \tag{55}$$

B. Components of the Class-DE$_M$ Tuned Power Amplifier

The output voltage v_O is

$$v_O = V_M\sin(\omega t) \tag{56}$$

where $V_M = RI_M$. And the fundamental component of the voltage across the inductor L_m is

$$v_L = V_{LM}\cos(\omega t) \tag{57}$$

where $V_{LM} = \omega L_m I_M$. Using the Fourier transform, the amplitude of the output voltage V_M is obtained from (51)

$$\begin{aligned} V_M &= \frac{1}{\pi}\int_0^{2\pi} v_{\mathrm{DS2}}\cdot\sin\omega t d(\omega t) \\ &= \frac{1}{\pi}\int_0^{\frac{\pi}{2}} V_{\mathrm{IN}}\cdot\sin\omega t d(\omega t) \\ &\quad + \frac{1}{\pi}\int_{\frac{\pi}{2}}^{\pi}\frac{3}{4}V_{\mathrm{IN}}\left(\cos\omega t+\frac{1}{3}\cos\omega_3 t+\frac{4}{3}\right)\sin\omega t d(\omega t) \\ &\quad + \frac{1}{\pi}\int_{\frac{3}{2}\pi}^{2\pi}\frac{3}{4}V_{\mathrm{IN}}\left(\cos\omega t+\frac{1}{3}\cos\omega_3 t\right)\sin\omega t d(\omega t) \\ &= \frac{3V_{\mathrm{IN}}}{2\pi}. \end{aligned} \tag{58}$$

Similarly, the amplitude of the inductor voltage V_{LM} is

$$\begin{aligned} V_{LM} &= \frac{1}{\pi}\int_0^{2\pi} v_{DS2}\cdot\cos\omega t d(\omega t) \\ &= \frac{1}{\pi}\int_0^{\frac{\pi}{2}} V_{\rm IN}\cdot\cos\omega t d(\omega t) \\ &\quad + \frac{1}{\pi}\int_{\frac{\pi}{2}}^{\pi}\frac{3}{4}V_{\rm IN}\left(\cos\omega t+\frac{1}{3}\cos\omega_3 t+\frac{4}{3}\right)\cos\omega t d(\omega t) \\ &\quad + \frac{1}{\pi}\int_{\frac{3\pi}{2}}^{2\pi}\frac{3}{4}V_{\rm IN}\left(\cos\omega t+\frac{1}{3}\cos\omega_3 t\right)\cos\omega t d(\omega t) \\ &= \frac{3V_{\rm IN}}{8}. \end{aligned} \tag{59}$$

From (58) and (59), we have

$$\frac{V_{LM}}{V_M} = \frac{\omega L_m I_M}{RI_M} = \frac{\omega L_m}{R} = \frac{\pi}{4}. \tag{60}$$

From (58), the output power P_O is

$$P_O = \frac{V_M^2}{2R} = \frac{9V_{\rm IN}^2}{8\pi^2 R}. \tag{61}$$

The injection power $P_{\rm aux}$ is changed by n, where n is the order of the harmonic component of the injection current. From [16, eq. (23)], $P_{\rm aux} = P_O/n^2$. This time, $n = 3$. The output power P_O is the sum of the input power $P_{\rm IN}$ and the injection power $P_{\rm aux}$.

$$P_O = P_{\rm IN} + P_{\rm aux} = P_{\rm IN} + \frac{1}{9}P_O = \frac{9}{8}P_{\rm IN}. \tag{62}$$

From (55) and (62), we have

$$P_O = \frac{9}{8}P_{\rm IN} = \frac{9}{8}I_{\rm IN}V_{\rm IN} = \frac{9}{8}\cdot\frac{\omega(C_{S1}+C_{S2})V_{\rm IN}^2}{2\pi}. \tag{63}$$

From (61) and (63), we have

$$\begin{aligned} \frac{\omega(C_{S1}+C_{S2})V_{\rm IN}^2}{2\pi} &= \frac{8}{9}\cdot\frac{9V_{\rm IN}^2}{8\pi^2 R}, \\ &\iff \omega(C_{S1}+C_{S2})R = \frac{2}{\pi}. \end{aligned} \tag{64}$$

From (36) and (64), the shunt capacitance C_S is

$$C_S = \frac{1}{\pi\omega R}. \tag{65}$$

With the loaded quality factor Q_1, the inductance L_f is expressed as

$$L_f = \frac{RQ_1}{\omega}. \tag{66}$$

From (60) and (66), the inductance L' is

$$L' = L_f - L_m = \left(Q_1 - \frac{\pi}{4}\right)\frac{R}{\omega}. \tag{67}$$

Thus, the capacitance C_f is

$$C_f = \frac{1}{\omega^2 L'} = \frac{1}{\omega R\left(Q_1 - \frac{\pi}{4}\right)}. \tag{68}$$

From (61), the load resistance R is

$$R = \frac{9V_{\rm IN}^2}{8\pi^2 P_O}. \tag{69}$$

C. Injection-Port Impedance for the Third-Order Harmonic

The injection-port impedance $Z_{\rm aux}$ (seen from the auxiliary circuit) can be obtained with the third-order harmonic component of the drain–source voltage $v_{\rm DS2}$. The injection-port impedance $Z_{\rm aux}$ is expressed by

$$Z_{\rm aux} = R_{\rm aux} + jX_{\rm aux} \tag{70}$$

where the reactance is $|X_{\rm aux}| = 1/(\omega_3 C_{\rm aux})$. The third-order harmonic component $v_{\rm DS2\_3}$ of the drain–source voltage $v_{\rm DS2}$ is

$$v_{\rm DS2\_3} = V_{M3}\sin(\omega_3 t+\phi_2) + V_{LM3}\cos(\omega_3 t+\phi_2) \tag{71}$$

where V_{M3} and V_{LM3} are Fourier coefficients obtained from (51)

$$\begin{aligned} V_{M3} &= \frac{1}{\pi}\int_0^{2\pi} v_{DS2}\cdot\sin(\omega_3 t+\pi)d(\omega t) \\ &= -\frac{1}{\pi}\int_0^{2\pi} v_{DS2}\cdot\sin\omega_3 t d(\omega t) \\ &= -\frac{1}{\pi}\int_0^{\frac{\pi}{2}} V_{\rm IN}\cdot\sin 3\omega t d(\omega t) \\ &\quad - \frac{1}{\pi}\int_{\frac{\pi}{2}}^{\pi}\frac{3}{4}V_{\rm IN}\left(\cos\omega t+\frac{1}{3}\cos 3\omega t+\frac{4}{3}\right)\sin 3\omega t d(\omega t) \\ &\quad - \frac{1}{\pi}\int_{\frac{3\pi}{2}}^{2\pi}\frac{3}{4}V_{\rm IN}\left(\cos\omega t+\frac{1}{3}\cos 3\omega t\right)\sin 3\omega t d(\omega t) \\ &= \frac{V_{\rm IN}}{6\pi} \end{aligned} \tag{72}$$

$$\begin{aligned} V_{LM3} &= \frac{1}{\pi}\int_0^{2\pi} v_{DS2}\cdot\cos(\omega_3 t+\pi)d(\omega t) \\ &= -\frac{1}{\pi}\int_0^{2\pi} v_{DS2}\cdot\cos\omega_3 t d(\omega t) \\ &= -\frac{1}{\pi}\int_0^{\frac{\pi}{2}} V_{\rm IN}\cdot\cos 3\omega t d(\omega t) \\ &\quad - \frac{1}{\pi}\int_{\frac{\pi}{2}}^{\pi}\frac{3}{4}V_{\rm IN}\left(\cos\omega t+\frac{1}{3}\cos 3\omega t+\frac{4}{3}\right)\cdot\cos 3\omega t d(\omega t) \\ &\quad - \frac{1}{\pi}\int_{\frac{3\pi}{2}}^{2\pi}\frac{3}{4}V_{\rm IN}\left(\cos\omega t+\frac{1}{3}\cos 3\omega t\right)\cdot\cos 3\omega t d(\omega t) \\ &= -\frac{V_{\rm IN}}{8} \end{aligned} \tag{73}$$

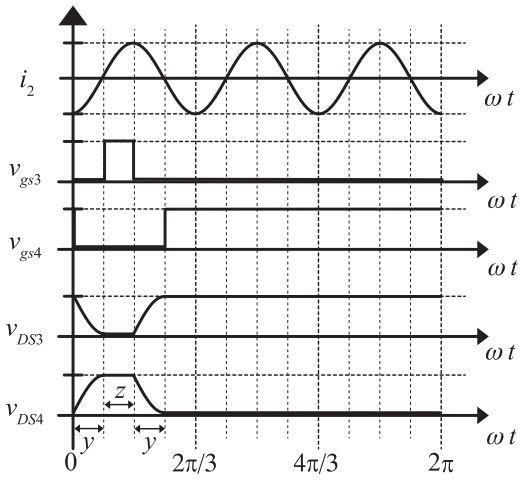

Fig. 3. Waveforms in the third-order Class-DE frequency multiplier.

The injection-port resistance $R_{\rm aux}$ and the reactance $X_{\rm aux}$ for the third-order harmonic component are

$$R_{\rm aux} = \frac{V_{M3}}{I_M} = \frac{V_{\rm IN}}{6\pi} \cdot \frac{4}{3\omega(C_{S1}+C_{S2})V_{\rm IN}} = \frac{2}{9\pi\omega(C_{S1}+C_{S2})} = \frac{V_{\rm IN}^2}{8\pi^2 P_O} = \frac{1}{9}R \tag{74}$$

$$X_{\rm aux} = \frac{V_{LM3}}{I_M} = -\frac{V_{\rm IN}}{8} \cdot \frac{4}{3\omega(C_{S1}+C_{S2})V_{\rm IN}} = \frac{-1}{6\omega(C_{S1}+C_{S2})}. \tag{75}$$

From (75), the injection-port capacitance $C_{\rm aux}$ is

$$C_{\rm aux} = \left|\frac{1}{\omega_3 X_{\rm aux}}\right| = 2(C_{S1}+C_{S2}). \tag{76}$$

D. Design Equations of the Class-DE Frequency Multiplier

The Class-DE frequency multiplier is analyzed in [27]. The frequency multiplier in the Class-DE$_{\rm M}$ amplifier is shown in Fig. 1(c). In [27], equations are derived for any order harmonic output current. In this study, we focus on the third-order harmonic current.

Fig. 3 shows waveforms in the third-order Class-DE frequency multiplier, where y is a duration of the dead time, and z is a duration while the switch S_3 is closed. To identify the equations with [27], waveforms in Fig. 3 are advanced by $3\pi/2$ from those in Fig. 2. In Fig. 3, the injection current i_2 is expressed as

$$i_2 = \frac{c}{R_{\rm aux}}\sin(3\omega t+\phi_2) \tag{77}$$

where c is the amplitude of the output voltage of the equivalent resistance $R_{\rm aux}$ and ϕ_2 is a phase angle. From [27, eq. (3)], the fundamental component of the drain–source voltage v_1 is

$$v_1 = v_O + v_L = c\sin(3\omega t+\phi_2) + \frac{c}{BR_{\rm aux}}\cos(3\omega t+\phi_2) = c_1\sin(3\omega t+\phi) \tag{78}$$

where v_O is the output voltage, v_L is the reactance voltage, and the parameter $B=\omega C_{S3}=\omega C_{S4}$ is the suceptance of the shunt capacitance, c_1 is

$$c_1 = c\sqrt{1+\frac{1}{(BR_{\rm aux})^2}} \tag{79}$$

and the phase difference ϕ is

$$\phi = \phi_2 + \arctan\left(\frac{1}{BR_{\rm aux}}\right). \tag{80}$$

When $y=z=\pi/6$, from [27, eq. (27)], the drain–source voltage $v_{\rm DS4}$ of the low-side switch S_4 is

$$v_{\rm DS4}(\omega t) = \begin{cases} \dfrac{c}{6BR_{\rm aux}}\left\{\cos(3\omega t+\phi_2)-\cos\phi_2\right\}, & \left[0<\omega t\le\dfrac{\pi}{6}\right] \\ V_{\rm IN2}, & \left[\dfrac{\pi}{6}<\omega t\le\dfrac{\pi}{3}\right] \\ V_{\rm IN2}+\dfrac{c}{6BR_{\rm aux}}\left\{\cos(3\omega t+\phi_2)+\cos\phi_2\right\}, & \left[\dfrac{\pi}{3}<\omega t\le\dfrac{\pi}{2}\right] \\ 0, & \left[\dfrac{\pi}{2}<\omega t\le 2\pi\right] \end{cases}. \tag{81}$$

From (78) and (81), the coefficient of the cos component is zero.

$$0 = \frac{1}{\pi}\int_0^{2\pi} v_{DS4}(\omega t)\cos(3\omega t+\phi)d(\omega t). \tag{82}$$

Solving (82) for c, we obtain

$$c = V_{\rm IN2}BR_{\rm aux}g(\phi_2,\phi). \tag{83}$$

g is given by [27, eqs. (15)–(17)]. The drain–source voltage $v_{\rm DS4}$ is $V_{\rm IN2}$ at $\omega t=\pi/6$. Therefore, from (81) and (83), we have

$$v_{\rm DS4}\left(\frac{\pi}{6}\right) = \frac{-gV_{\rm IN2}}{6}\left(\sin\phi_2+\cos\phi_2\right) = V_{\rm IN2}. \tag{84}$$

To satisfy (84), $g\neq 0$ is needed. From [27, eq. (28)], the normalized slope ζ of the drain–source voltage $v_{\rm DS4}$ is zero at $\omega t=\pi/6$.

$$\zeta = \frac{1}{V_{\rm IN2}}\frac{d}{d(\omega t)}v_{\rm DS4}(\omega t)\bigg|_{\omega t=\frac{\pi}{6}} = -\frac{g}{2}\sin\left(\frac{\pi}{2}+\phi_2\right) = 0. \tag{85}$$

From (85) and $g\neq 0$, the phage angle $\phi_2=-\pi/2$ is determined. Thus, from (84), the parameter $g=6$ is determined.

Substituting $y=z=\pi/6$ and $\phi_2=-\pi/2$ into [27, eq. (30)], we obtain

$$B = \frac{1}{6\pi gR_{\rm aux}}\left[\cos\phi_2+\cos(3y+\phi_2) - \cos(3y+3z+\phi_2)-\cos(6+3z+\phi_2)\right] = \frac{1}{18\pi R_{\rm aux}}. \tag{86}$$

From [27, eqs. (5) and (31)–(33)] and (80), the reactance X is

$$X = \frac{\pi}{2}R_{\rm aux} \tag{87}$$

where $X = \omega_3 L_{m2}$. From [27, eq. (23)], we have

$$P_{\rm aux} = \frac{V_{\rm IN2}^2}{18\pi^2 R_{\rm aux}} \tag{88}$$

where $P_{\rm aux}$ is the injection power. The inductor L_{f2} is

$$L_{f2} = \frac{Q_2 R_{\rm aux}}{\omega_3}. \tag{89}$$

From (87), the inductor L_2' is

$$L_2' = L_{f2} - L_{m2} = \left(Q_2 - \frac{\pi}{2}\right)\frac{R_{\rm aux}}{\omega_3}. \tag{90}$$

Since L_2'–C_m is tuned to $3f$, the capacitor C_m is

$$C_m = \frac{1}{\omega_3^2 L_2'} = \frac{1}{\omega_3 R_{\rm aux}\left(Q_2 - \frac{\pi}{2}\right)}. \tag{91}$$

The capacitor C_m can be regarded as a series connection of the capacitor C_{f2} and the capacitor $C_{\rm aux}$.

$$C_{f2} = \frac{C_{\rm aux} C_m}{C_{\rm aux} - C_m}. \tag{92}$$

From (62) and (88), we have

$$P_{\rm aux} = \frac{1}{9}P_O, \iff \frac{V_{\rm IN2}^2}{18\pi^2 R_{\rm aux}} = \frac{V_{\rm IN}^2}{8\pi^2 R}. \tag{93}$$

Finally, considering (74), we get the relation $V_{\rm IN} = 2V_{\rm IN2}$.

E. Switch Voltage and Current Stresses of the Class-DE$_M$ Amplifier

The voltage stresses V_{S1} and V_{S2} of switches S_1 and S_2 are equal to the input voltage $V_{\rm IN}$:

$$V_{S1} = V_{S2} = V_{\rm IN}. \tag{94}$$

Since the slope at the peak of the switch current is 0, differentiating (52) yields

$$\frac{di_{S1}}{d(\omega t)} = I_M(\cos\omega t + 3\cos\omega_3 t) = 0. \tag{95}$$

From (95), $\cos\omega t = 0$, $\pm\sqrt{2/3}$ are obtained. When the current has a peak value, $\cos\omega t = \pm\sqrt{2/3}$, or $\sin\omega t = \pm\sqrt{1/3}$. Substituting $\sin\omega t = \sqrt{1/3}$ into (52), the current stress of the switch I_{S1} is

$$\begin{aligned} I_{S1} &= I_M(\sin\omega t + \sin 3\omega t) \\ &= I_M(4\sin\omega t - 4\sin^3\omega t) = \frac{8\sqrt{3}}{9}I_M \\ &= \frac{2\sqrt{3}\omega(C_{S1}+C_{S2})V_{\rm IN}}{3}. \end{aligned} \tag{96}$$

Also, for the switch S_2, it is the same value.

III. Design of the Class-DE$_{\rm M}$ Tuned Power Amplifier

Initial conditions of the Class-DE$_{\rm M}$ tuned power amplifier is given as follows.

1) The output power $P_O = 5.00$ W.
2) The operating frequency $f = 1.00$ MHz.
3) The load resistance $R = 50\ \Omega$.
4) The load quality factors of the main circuit $Q_1 = 5$ and the injection circuit $Q_2 = 30$.

From (69), the input voltage of the main circuit $V_{\rm IN}$ is

$$V_{\rm IN} = \sqrt{\frac{8\pi^2 P_O R}{9}} = 46.8\ \text{V}. \tag{97}$$

Therefore, the input voltage of the auxiliary circuit is $V_{\rm IN2} = 23.4$ V. The drain-to-source capacitance of the MOSFET (IRFR120Z) $C_{\rm ds}$ is 17 [pF] [28]. From (65), the shunt capacitances are

$$C_{S1} = C_{S2} = \frac{1}{\pi\omega R} - C_{\rm ds} = 996\ \text{pF}. \tag{98}$$

From (66), the resonant inductance L_f is

$$L_f = \frac{RQ_1}{\omega} = 39.8\ \mu\text{H}. \tag{99}$$

From (68), the resonant capacitance C_f is

$$C_f = \frac{1}{\omega R\left(Q_1 - \frac{\pi}{4}\right)} = 755\ \text{pF}. \tag{100}$$

From (74), the input resistance $R_{\rm aux}$ is

$$R_{\rm aux} = \frac{1}{9}R = 5.56\ \Omega. \tag{101}$$

From (75), the input reactance $|X_{\rm aux}|$ is

$$|X_{\rm aux}| = \left|\frac{-1}{6\omega(C_{S1}+C_{S2})}\right| = 13.1\ \Omega. \tag{102}$$

Therefore, $C_{\rm aux} = 4.05$ nF. From (86), the shunt capacitances C_{S3} and C_{S4} are

$$C_{S3} = C_{S4} = \frac{1}{18\pi\omega R_{\rm aux}} - C_{\rm ds} = 490\ \text{pF}. \tag{103}$$

From (89), the resonant inductance L_{f2} is

$$L_{f2} = \frac{Q_2 R_{\rm aux}}{\omega_3} = 8.85\ \mu\text{H}. \tag{104}$$

From (91), the capacitance C_m is

$$C_m = \frac{1}{\omega_3 R_{\rm aux}\left(Q_2 - \frac{\pi}{2}\right)} = 336\ \text{pF}. \tag{105}$$

From (92) and (105), the resonant capacitance C_{f2} is

$$C_{f2} = \frac{C_{\rm aux} C_m}{C_{\rm aux} - C_m} = 366\ \text{pF}. \tag{106}$$

From (96), the current stresses I_{S1} and I_{S2} of switches S_1 and S_2 are

$$I_{S1} = I_{S2} = \frac{2\sqrt{3}\omega(C_{S1}+C_{S2})V_{\rm IN}}{3} = 0.689\ \text{A} \tag{107}$$

which is smaller than the absolute maximum rating of the drain current of the MOSFET IRFR120Z [28].

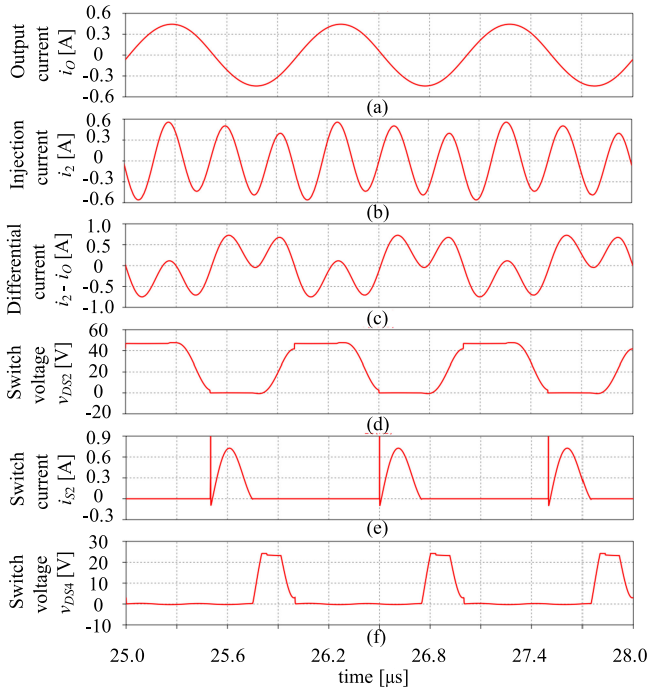

Fig. 4. Simulation waveforms under the ideal condition (the load quality factor $Q_2 = 30$). (a) Output current i_O. (b) Injection current i_2. (c) Differential current i_2–i_O. (d) Switch current i_{S2}. (e) Drain–source voltage $v_{\rm DS2}$. (f) Switch current i_{S2}. (g) Drain–source voltage $v_{\rm DS4}$.

IV. Simulation Results

To confirm the operation of the designed circuit, the designed Class-DE$_{\rm M}$ tuned power amplifier was simulated with LTspice IV for OS X under the ideal condition. In this simulation, ESRs of all the passive components were zero, and the switches were assumed to be ideal. The simulation waveforms are shown in Fig. 4. In Fig. 4(b) and (c), the injection current i_2 and the differential current i_2–i_O are distorted. The reasons of the current distortion of i_2 could be that the injection-port impedance is defined as a fixed impedance; however, it is time varying, and that the Q_2 was low for a frequency multiplier. Therefore, the switch current i_{S2} does not satisfy ZCS at turning-ON in Fig. 4(e). And, a spike current is caused by the slight remaining voltage of the drain–source voltage $v_{\rm DS2}$. In Fig. 4(d), the drain–source voltage $v_{\rm DS2}$ almost satisfies ZVS and ZVDS at both turning-ON and turning-OFF. In Fig. 4(f), the drain–source voltage $v_{\rm DS4}$ does not satisfy ZVS or ZVDS. This is also caused by the current distortion of i_2.

V. Circuit Experiment

To confirm the circuit operation, a Class-DE$_{\rm M}$ tuned power amplifier was built and tested. A picture of the experimental circuit is shown in Fig. 5. Experimental parameters are shown in Table I. In the series-resonant circuit L_f–C_f and L_{f2}–C_{f2}, the loaded quality factors Q_1, Q_2 and the resonant inductances L_f and L_{f2} were adjusted according to the capacitances C_f and C_{f2}. T130-2 [29] was used for the cores of the inductors L_f and L_{f2}. The measured voltages, currents, and powers are shown in Table II, where the theoretical values and simulation results

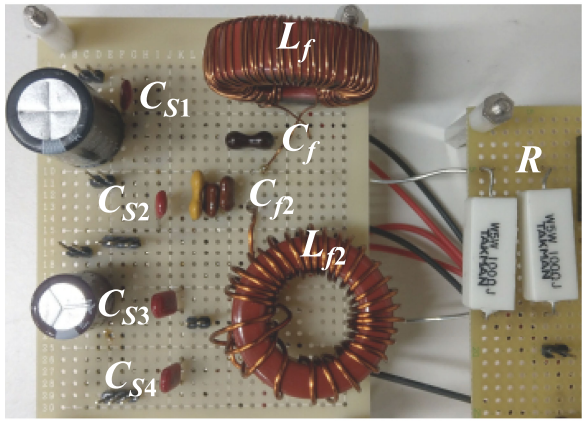

Fig. 5. Experimental circuit.

TABLE I
Experimental Parameters

	Theory (ESR [Ω])	Measured [%]	Difference
C_{S1} [nF]	0.996	1.01 (0.0971)*	+1.41
C_{S2} [nF]	0.996	1.03 (0.111)*	+3.41
L_f [μH]	39.8	37.2 (0.621)*	–
C_f [nF]	0.755	0.816 (0.015)*	–
R [Ω]	50	50*	0
C_{S3} [nF]	0.490	0.457 (0.222)**	−6.73
C_{S4} [nF]	0.490	0.465 (0.231)**	−5.10
L_{f2} [μH]	8.84	9.18 (0.870)**	–
C_{f2} [nF]	0.366	0.351 (0.230)**	–

* Measured at 1 MHz by the LCR meter (HIOKI IM3536).
** Measured at 3 MHz.

TABLE II
Experimental and Simulation Results

	Theory	Measured	Sim. (exp.)
$V_{\rm IN}$ [V]	46.8	46.8	46.8
$V_{\rm IN2}$ [V]	23.4	23.4	23.4
$I_{\rm IN}$ [mA]	94.9	97.5	97.5
$I_{\rm IN2}$ [mA]	23.7	27.8	27.7
$P_{\rm IN}$ [W]	4.44	4.57	4.56
$P_{\rm IN2}$ [W]	0.556	0.655	0.648
$I_{O\rm rms}$ [mA]	316	312**	298
$I_{2\rm rms}$ [mA]	316	267**	284
I_O [mA]	447	441**	420
I_2 [mA]	447	378**	401
$V_{O\rm rms}$ [V]	15.8	15.6	15.7
P_O [W]	5	4.87	4.93
η [%]	92.6*	93.2	94.6

* Considered the overall power losses (B1) derived from Appendix B (used the measured current value).
** Calculated from the output voltage or inductor voltage.

under the experimental condition are also shown. ESRs of all the passive components and on-resistance of the switches were taken into consideration for the simulation. $I_{O\rm rms}$ and $I_{2\rm rms}$ mean the RMS values of the currents through the inductors L_f and L_{f2}. $I_{O\rm rms}$ and I_O are calculated from the output voltage and the load resistance R. And, $I_{2\rm rms}$ and I_2 are calculated from the measured inductor voltage $v_{\rm Lf2}$ and $3\omega L_{f2}$.

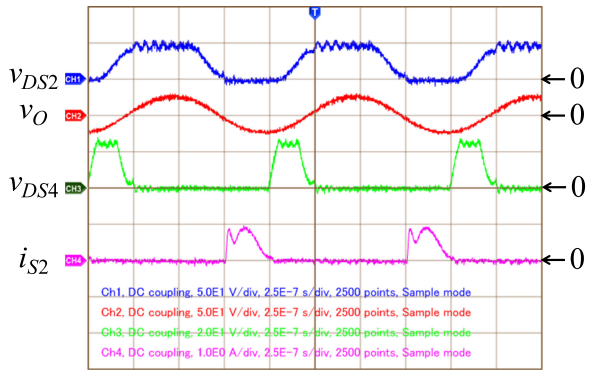

Fig. 6. Experimental waveforms of the drain–source voltage v_{DS2}, the output voltage v_O, the drain–source voltage v_{DS4}, and the switch current i_{S2}, v_{DS2}, and v_O : 50 V/div, v_{DS4} : 20 V/div, i_{S2} : 1 A/div, horizontal: 0.25 μs/div.

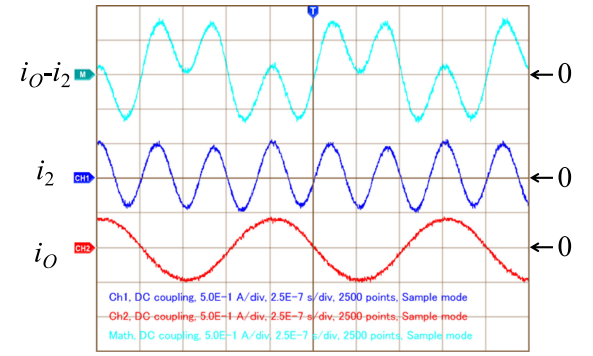

Fig. 7. Experimental waveforms of the differential current i_2–i_O, the injection current i_2, and the output current i_O, i_2–i_O, i_2, and i_O : 0.5 A/div, horizontal: 0.25 μs/div.

Observed waveforms of the drain–source voltage v_{DS2}, the output voltage v_O, the drain–source voltage v_{DS4}, and the switch current i_{S2} are shown in Fig. 6. The output voltage v_O was in sinusoidal waveform, whose RMS value $V_{O\mathrm{rms}}$ was 15.6 V. The drain–source voltage v_{DS2} achieved ZVS and ZVDS at turning-ON and turning-OFF. And the switch current i_{S2} achieved ZCS at turning-ON, ZCS and ZCDS at turning-OFF. However, the drain–source voltage v_{DS4} did not achieve ZVS or ZVDS, which agreed with the simulation results in Section IV.

Observed waveforms of the differential current i_2–i_O, the injection current i_2, and the output current i_O are shown in Fig. 7. The output current i_O was in sinusoidal waveform without distortion. However, the injection current i_2 was slightly distorted, and the fundamental component was dominant. Distortion of the waveform of the injection current i_2 affects i_2–i_O.

The power conversion efficiency of the amplifier is calculated as

$$\eta = \frac{P_O}{P_{\mathrm{IN}} + P_{\mathrm{IN2}}} \tag{108}$$

where P_O is the output power, P_{IN} is the input power of the main circuit, and P_{IN2} is the input power of the auxiliary circuit. From Table II, the power conversion efficiency in the simulation was 94.6%. The theoretical efficiency obtained from (B1) is 95.4%. The difference between the simulation efficiency and the theoretical efficiency could be caused by the core power loss. The measured power conversion efficiency was 93.2%, which was lower than the theoretical and the simulation values. The difference between the simulation efficiency and the theoretical efficiency could be caused by the distortion of the injection current i_2 and the parasitic resistance in the circuit. Both the measured input currents I_{IN} and I_{IN2} were slightly larger than the theory. It could be caused by the deviation of the resonant frequency of the resonant circuits L_f–C_f and L_{f2}–C_{f2}.

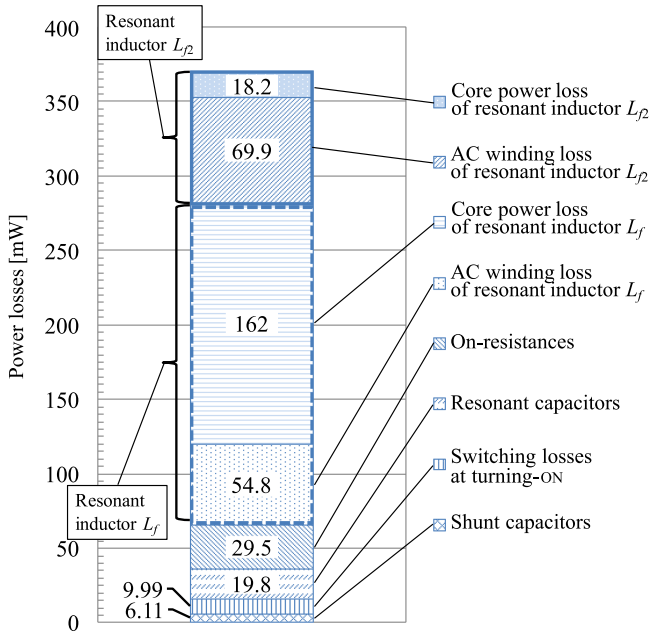

Fig. 8. Theoretical power loss breakdown of the Class-DE$_{\mathrm{M}}$ amplifier (P_O = 5 W).

Theoretical power losses breakdown of the Class-DE$_{\mathrm{M}}$ amplifier is shown in Fig. 8. From Fig. 8, the proportion occupied by the conduction losses of the resonant inductors L_f and L_{f2} is larger than that of the switching losses at turning-ON. The power conversion efficiency would be further improved by reducing inductor losses.

VI. Conclusion

The Class-DE$_{\mathrm{M}}$ tuned power amplifier has been proposed. The Class-DE$_{\mathrm{M}}$ amplifier achieves ZVS and ZVDS at the turning-ON and turning-OFF. Moreover, the switch current satisfies ZCS at turning-ON and turning-OFF, and ZCDS at turning-OFF, which decrease the switching losses. The voltage stress of the switches is low, which is no more than the input voltage. The auxiliary circuit needs a voltage source, which supplies a half voltage of the input voltage. The circuit operation has been verified with the simulation and the circuit experiments. The experimental results showed good agreement with the theory and the simulation results. In the circuit experiments of the proposed amplifier, the power conversion efficiency was 93.2% with the output power of 4.87 W at 1.0 MHz.

APPENDIX A
VOLTAGE STRESS OF THE CLASS-E$_{\rm M}$ TUNED POWER AMPLIFIER

When $n = 2$, meaning that the injection current frequency is the second harmonic, from [16, eq. (31)], the drain–source voltage v_S of the Class-E$_{\rm M}$ amplifier is

$$v_S(\omega t) = \frac{I_O}{16\pi f C_\infty}\left(8\omega t + 4\pi\cos\omega t - \pi\cos 2\omega t - 4\sin 2\omega t - 3\pi\right), \quad [\pi \leqq \omega t \leqq 2\pi] \tag{A1}$$

where $\omega = 2\pi f$ is the angular time and f is the fundamental frequency, I_0 is the dc input current, and C_∞ is the shunt capacitance. Since the slope at the peak of the drain–source voltage becomes 0 at $t = t_p$, differentiating (A1) yields

$$\left.\frac{dv_S(\omega t)}{d\omega t}\right|_{\omega t=\omega t_p} = \frac{I_O}{16\pi f C_\infty}\left(8 - 4\pi\sin\omega t_p + 2\pi\sin 2\omega t_p - 8\cos 2\omega t_p\right) = 0. \tag{A2}$$

Solving (A2) for $\sin\omega t_p$, we obtain

$$\sin\omega t_p = \frac{\dfrac{8}{\pi}}{1+\dfrac{16}{\pi^2}}. \tag{A3}$$

From [16, Table I], the shunt capacitance C_∞ is

$$C_\infty = \frac{3}{128}\frac{P_{\rm OUT}}{V_{\rm DC}^2 f} \tag{A4}$$

where $P_{\rm OUT}$ is the output power and $V_{\rm DC}$ is the input voltage. From [16, Table I], the dc input current is

$$I_O = \frac{3}{4}\frac{P_{\rm OUT}}{V_{\rm DC}}. \tag{A5}$$

From (A1)–(A5), the normalized drain–source voltage stress $V_{\rm SM}/V_{\rm DC}$ is

$$\frac{V_{\rm SM}}{V_{\rm DC}} \simeq 4.27. \tag{A6}$$

From [27], the normalized voltage stress of the Class-E amplifier is $V_{\rm SM}/V_{\rm DC} = 3.56$ ($D = 0.5$). Therefore, the Class-E$_{\rm M}$ amplifier ($n = 2$) has the voltage stress approximately 1.20 times compared with that of the Class-E amplifier.

APPENDIX B
POWER CONVERSION EFFICIENCY

The power conversion efficiency of the amplifier is

$$\eta = \frac{P_O}{P_O + P_{\rm loss}} \tag{B1}$$

where P_O is the output power and $P_{\rm loss}$ is the overall power losses, which is given as

$$P_{\rm loss} = P_{S1} + P_{S2} + P_{S3} + P_{S4} + P_{\rm rCS1} + P_{\rm rCS2} + P_{\rm rCS3} + P_{\rm rCS4} + P_{\rm rLf} + P_{\rm rLf2} + P_{\rm rCf} + P_{\rm rCf2} + P_{\rm core} + 4P_{t\_\rm on} \tag{B2}$$

where P_{S1}–P_{S4} are the switch conduction losses, $P_{\rm rCS1}$, $P_{\rm rCS2}$, $P_{\rm rCS3}$, $P_{\rm rCS4}$, $P_{\rm rLf}$, $P_{\rm rLf2}$, $P_{\rm rCf}$, and $P_{\rm rCf2}$ are the power losses in the ESR $r_{\rm CS1}$, $r_{\rm CS2}$, $r_{\rm CS3}$, and $r_{\rm CS4}$ of shunt capacitors, $r_{\rm Lf}$ and $r_{\rm Lf2}$ of the resonant inductors, $r_{\rm Cf}$ and $r_{\rm Cf2}$ of the resonant capacitors, $P_{\rm core}$ is the core power loss of the inductors L_f and L_{f2}, and $P_{t\_\rm on}$ is the switching losses at the turning-ON.

1) Conduction Power Losses of Switches S_1–S_4: From (52), the RMS value of the switch current $I_{S1\rm rms}$ is

$$I_{S1\rm rms} = \sqrt{\frac{1}{2\pi}\int_0^{2\pi} i_{S1}^2 d(\omega t)} = \frac{I_M}{2}. \tag{B3}$$

Therefore, using (B3), the switch conduction loss P_{S1} is

$$P_{S1} = r_{\rm ON} I_{S1\rm rms}^2 = \frac{r_{\rm ON} I_M^2}{4} \tag{B4}$$

where $r_{\rm ON}$ is the switch on-resistance. Also, for switch S_2, P_{S2} has the same value.

The RMS values of the switch currents $I_{S3\rm rms}$ and $I_{S4\rm rms}$ are

$$I_{S3\rm rms} = \sqrt{\frac{1}{2\pi}\int_0^{2\pi} i_{S3}^2 d(\omega t)} = \sqrt{\frac{1}{2\pi}\int_{5\pi/3}^{11\pi/6} (-I_M\sin 3\omega t)^2 d(\omega t)} = \frac{1}{2}\sqrt{\frac{1}{6}} I_M \tag{B5}$$

$$I_{S4\rm rms} = \sqrt{\frac{1}{2\pi}\int_0^{2\pi} i_{S4}^2 d(\omega t)} = \sqrt{\frac{1}{2\pi}\int_0^{3\pi/2} (I_M\sin 3\omega t)^2 d(\omega t)} = \frac{1}{2}\sqrt{\frac{3}{2}} I_M. \tag{B6}$$

From (B5) and (B6), the switch conduction losses P_{S3} and P_{S4} are

$$P_{S3} = r_{\rm ON} I_{S3\rm rms}^2 = \frac{r_{\rm ON} I_M^2}{24} \tag{B7}$$

$$P_{S4} = r_{\rm ON} I_{S4\rm rms}^2 = \frac{3 r_{\rm ON} I_M^2}{8}. \tag{B8}$$

2) Power Losses in the ESR $r_{\rm CS1}$–$r_{\rm CS4}$ of the Shunt Capacitors:

The RMS value of the shunt capacitor current $I_{\rm CS1rms}$ is

$$I_{\rm CS1rms} = \sqrt{\frac{1}{2\pi}\int_0^{2\pi} i_{\rm CS1}^2 d(\omega t)} = \frac{1}{2}\sqrt{\frac{1}{2}} I_M. \tag{B9}$$

From (B9), the power loss $P_{\rm rCS1}$ is

$$P_{\rm rCS1} = r_{\rm CS1} I_{\rm CS1rms}^2 = \frac{r_{\rm CS1} I_M^2}{8}. \tag{B10}$$

For the shunt capacitor C_{S2}, the power loss $P_{\rm rCS2}$ has the same value.

The RMS value of the shunt capacitor current I_{CS3rms} is

$$I_{\mathrm{CS3rms}} = \sqrt{\frac{1}{2\pi}\int_0^{2\pi} i_{\mathrm{CS3}}^2 d(\omega t)} = \sqrt{\frac{1}{2\pi}\int_{3\pi/2}^{5\pi/3}\left(-\frac{I_M}{2}\sin 3\omega t\right)^2 d(\omega t)} + \sqrt{\frac{1}{2\pi}\int_{11\pi/6}^{2\pi}\left(-\frac{I_M}{2}\sin 3\omega t\right)^2 d(\omega t)} = \frac{1}{4}\sqrt{\frac{1}{3}} I_M. \tag{B11}$$

From (B11), the power loss P_{rCS3} is

$$P_{\mathrm{rCS3}} = r_{\mathrm{CS3}} I_{\mathrm{CS3rms}}^2 = \frac{r_{\mathrm{CS3}} I_M^2}{48}. \tag{B12}$$

The same equations are applied to the shunt capacitor C_{S4}.

3) Power Losses in ESRs $\mathrm{r_{Lf}}$, $\mathrm{r_{Lf2}}$, $\mathrm{r_{Cf}}$, *and* $\mathrm{r_{Cf2}}$*:* The power loss in the ESR r_{Lf} of the resonant inductor L_f is

$$P_{\mathrm{rLf}} = r_{\mathrm{Lf}} \frac{I_M^2}{2}. \tag{B13}$$

The power loss in the ESR r_{Cf} of the resonant capacitor C_f is

$$P_{\mathrm{rCf}} = r_{\mathrm{Cf}} \frac{I_M^2}{2}. \tag{B14}$$

The output current i_O and the injection current i_2 have the same amplitude, i.e., their RMS values are also the same. Therefore, the power losses in the ESR r_{Lf2} of the resonant inductor L_{f2} and in the ESR r_{Cf2} of the resonant capacitor C_{f2} are similarly derived.

4) Core Power Losses in the Inductors $\mathrm{L_f}$ *and* $\mathrm{L_{f2}}$*:* From [29], the core power loss density CL of T130-2 is calculated with

$$CL[\mathrm{mW/cm^3}] = \frac{f}{\dfrac{a}{B_m^3} + \dfrac{b}{B_m^{2.3}} + \dfrac{c}{B_m^{1.65}}} + df^2 B_m^2 \tag{B15}$$

where $a = 4.0 \times 10^9$, $b = 3.0 \times 10^8$, $c = 2.7 \times 10^6$, and $d = 8.0 \times 10^{-15}$ are constants for core material, f is frequency, and B_m [G] is the maximum magnetic flux density. The core power loss density CL contains hysteresis and eddy-current core loss. The maximum magnetic flux density B_m is given by

$$B_m = \frac{\Delta I L}{2 A_C N} \times 10^4 \ [\mathrm{G}] \tag{B16}$$

where ΔI [A] is the peak-to-peak current through an inductance L [H], A_C [$\mathrm{m^2}$] is the cross-sectional area, and N [turns] is the number of turns. The core power loss P_{core} [mW] is

$$P_{\mathrm{core}} = CL \times V_C \tag{B17}$$

where V_C [$\mathrm{cm^3}$] is the volume of the core. Parameters for core power losses are shown in Table III.

5) Power Losses of the Switch at Turning-ON: As shown in Fig 6, v_{DS2} and v_{DS4} did not achieve ZVS. And the voltages at turning-ON were equality $V_{\mathrm{ON}} = 6.0$ [V]. From [28], the drain–source capacitance $C_{\mathrm{ds(25V)}}$ is 17 pF. From [2, eq. (6.87)], the switching loss at turning-ON is given by

$$P_{t\_\mathrm{on}} = 10 f C_{\mathrm{ds(25V)}} \sqrt{V_{\mathrm{ON}}^3}. \tag{B18}$$

TABLE III
PARAMETERS FOR CORE POWER LOSSES

	L_f	L_{f2}
Peak-to-peak current ΔI [mA]	882*	755*
Inductance L [μH]	37.2*	9.18*
Number of turns N [turns]	51	29
Cross-sectional area A_C [$\mathrm{cm^2}$]	0.698	0.698
Volume of the core V_C [$\mathrm{cm^3}$]	0.110	0.110
Maximum magnetic flux density B_m [G]	46.1	17.1
Core power loss density CL [$\mathrm{mW/cm^3}$]	25.2	3.58
Core power loss P_{core} [mW]	162	18.2

*Measured values.

REFERENCES

[1] A. Grebennikov and N. O. Sokal, *Switchmode RF Power Amplifiers*. New York, NY, USA: Newnes, 2007.

[2] M. K. Kazimierczuk and D. Czarkowski, *Resonant Power Converter*, 2nd ed. Hoboken, NJ, USA: Wiley, 2011.

[3] M. K. Kazimierczuk and J. S. Modzelewski, "Drive-transformerless Class-D voltage-switching tuned power amplifier," *Proc. IEEE*, vol. 68, no. 6, pp. 740–741, Jun. 1980.

[4] M. K. Kazimierczuk, "Class D voltage-switching MOSFET power amplifier," *Proc. IEE B, Electr. Power Appl.*, vol. 138, no. 6, pp. 285–296, Nov. 1991.

[5] M. K. Kazimierczuk and W. Szaraniec, "Class D voltage-switching inverter with only one shunt capacitor," *Proc. IEE B, Electr. Power Appl.*, vol. 139, pp. 449–456, Sep. 1992.

[6] S. A. El-Hamamsy, "Design of high-efficiency RF Class-D power amplifier," *IEEE Trans. Power Electron.*, vol. 9, no. 3, pp. 297–308, May 1994.

[7] N. O. Sokal and A. D. Sokal, "High efficiency tuned switching power amplifier," U.S. Patent no. 3 919 656, Nov. 11, 1975.

[8] J. Ebert and M. Kazimierczuk, "High efficiency RF power amplifier," *Bull. Polish Acad. Sci. Ser. Sci. Techn.*, vol. 25, no. 2, pp. 13–16, Feb. 1977.

[9] D. J. Kessler and M. K. Kazimierczuk, "Power losses and efficiency of Class-E power amplifier at any duty ratio," *IEEE Trans. Circuits Syst. I, Reg. Papers*, vol. 51. no. 9, pp. 1675–1689, Sep. 2004.

[10] N. Sokal and A. Sokal, "Class E—A new class of high-efficiency tuned single-ended switching power amplifiers," *IEEE J. Solid-State Circuits*, vol. SSC-10, no. 3, pp. 168–176, Jun. 1975.

[11] F. H. Raab, "Idealized operation of Class-E tuned power-amplifier," *IEEE Trans. Circuits Syst.*, vol. CAS-24, no. 12, pp. 725–735, Dec. 1977.

[12] F. H. Raab and N. O. Sokal, "Transistor power losses in the Class E tuned power amplifier," *IEEE J. Solid-State Circuits*, vol. SSC-13, no. 6, pp. 912–914, Dec. 1978.

[13] H. Koizumi, M. Fujii, K. Shinoda, T. Suetsugu, and S. Mori, "Phase-controlled class DE inverter," in *Proc. IEEE Int. Telecommun. Energy Conf.*, Oct. 1995, pp. 86–92.

[14] H. Koizumi, T. Suetsugu, M. Fujii, K. Shinoda, S. Mori, and K. Ikeda, "Class DE high-efficiency tuned power amplifier," *IEEE Trans. Circuits Syst. I, Fundam. Theory Appl.*, vol. 43, no. 1, pp. 51–60, Jan. 1996.

[15] M. Albulet, "An exact analysis of class-DE amplifier at any output Q," *IEEE Trans. Circuits Syst. I, Fundam. Theory Appl.*, vol. 46, no. 10, pp. 242–248, Apr. 1999.

[16] A. Telegdy, B. Molnár, and N. O. Sokal, "Class-$\mathrm{E_M}$ switching-mode tuned power amplifier-high efficiency with slow-switching transistor," *IEEE Trans. Microw. Theory Tech.*, vol. 51, no. 6, pp. 1662–1676, Jun. 2003.

[17] R. Miyahara, H. Sekiya, and M. K. Kazimierczuk, "Design of class-$\mathrm{E_M}$ power amplifier taking into account auxiliary circuit," in *Proc. Annu. Conf. IEEE Ind. Electron. Soc.*, Orlando, FL, USA, Nov. 2008, pp. 679–684.

[18] R. Miyahara, H. Sekiya, and M. K. Kazimierczuk, "Novel design procedure of class-$\mathrm{E_M}$ power amplifiers," *IEEE Trans. Microw. Theory Techn.*, vol. 58, no. 12, pp. 3607–3616, Dec. 2010.

[19] X. Wei, T. Nagashima, S. Kuroiwa, and H. Sekiya, "Design of symmetric class-E$_M$ power amplifier," in *Proc. 37th Annu. Conf. IEEE Ind. Electron. Soc.*, Melbourne, VIC, Australia, Nov. 2011, pp. 1300–1305.
[20] X. Wei, S. Kuroiwa, T. Nagashima, M. K. Kazimierczuk, and H. Sekiya, "Push-pull class-E$_M$ power amplifier for low harmonic-contents and high output-power applications," *IEEE Trans. Circuits Syst. I, Reg. Papers*, vol. 56, no. 9, pp. 2137–2146, Sep. 2012.
[21] R. Miyahara, X. Wei, T. Nagashima, T. Kousaka, and H. Sekiya, "Design of class-E$_M$ oscillator with second harmonic injection," *IEEE Trans. Circuits Syst. I, Reg. Papers*, vol. 59, no, 10, pp. 2456–2567, Oct. 2012.
[22] X. Wei, S. Kuroiwa, T. Nagashima, M. K. Kazimierczuk, and H. Sekiya, "Push-pull class-E$_M$ power amplifier for low harmonic-contents and high output-power applications," *IEEE Trans. Circuits Syst. I, Reg. Papers*, vol. 59, no. 9, pp. 2137–2146, Sep. 2012.
[23] X. Wei, T. Nagashima, M. K. Kazimierczuk, H. Sekiya, and T. Suetsugu, "Analysis and design of class-E$_M$ power amplifier," *IEEE Trans. Circuits Syst. I, Reg. Papers*, vol. 61, no. 4, pp. 976–986, Apr. 2014.
[24] R. E. Zulinski and J. W. Steadman, "Performance evaluation of class E frequency multiplier," *IEEE Trans. Circuits Syst.*, vol. CAS-33, no. 3, pp. 343–346, Mar. 1986.
[25] R. E. Zulinski and J. W. Steadman, "Idealized operation of class E frequency multiplier," *IEEE Trans. Circuits Syst.*, vol. CAS-33, no. 3, pp. 1209–1218, Dec. 1986.
[26] M. Albulet, "Analysis and design of the class E frequency multipliers with RF choke," *IEEE Trans. Circuits Syst. I, Fundam. Theory Appl.*, vol. 42, no. 2, pp. 95–104, Feb. 1995.
[27] K. Shinoda, T. Suetsugu, M. Matsuo, and S. Mori, "Idealized operation of Class DE amplifier and frequency multipliers," *IEEE Trans. Circuits Syst. I, Fundam. Theory Appl.*, vol. 45, no. 1, pp. 34–40, Jan. 1998.
[28] IRFR120Z date-sheet. [Online]. Available: http://www.irf.com/product-info/datasheets/data/irfr120z.pdf
[29] T130-2 date-sheet. [Online]. Available: http://www.micrometals.com/pcparts/pc_l.pdf

Tsuyoshi Inaba (S'16) received the B.E. degree in electrical engineering from the Tokyo University of Science, Tokyo, Japan, in 2016, where he is currently working toward the M.E. degree.

His research interests include high-frequency inverters and resonant dc/dc power converters.

Hirotaka Koizumi (S'98–M'01) was born in Tokyo, Japan, in 1970. He received the B.E., M.E., and Ph.D. degrees in electrical engineering from Keio University, Yokohama, Japan, in 1993, 1995, and 2001, respectively.

From 1995 to 2001, he was an Electrical Engineer with Tokyo Electric Power Company Inc., Tokyo. From 1998 to 2001, he was with the Graduate School, Keio University. From 2001 to 2007, he was a Research Associate with the Tokyo University of Agriculture and Technology, Tokyo. Since April 2007, he has been with the Tokyo University of Science, Tokyo, where he is currently a Professor. His research interests include photovoltaic systems, high-frequency high-efficiency tuned power amplifiers, resonant dc/dc power converters, dc/ac inverters, and high-frequency rectifiers.

Dr. Koizumi is a member of the Institute of Electrical Engineers of Japan and the Institute of Electronics, Information, and Communication Engineers of Japan. From May 2008 to May 2010, he was the Secretary of the Power Systems and Power Electronic Circuits Technical Committee of the IEEE Circuits and Systems Society. From May 2012 to May 2013 and from May 2013 to May 2014, he was the Chair and the Past Chair of the Power and Energy Circuits and Systems Technical Committee of the IEEE Circuits and Systems Society.